Guoyu Qian*, Guoguang Cheng and Zibing Hou

The Influence of the Induced Ferrite and Precipitates of Ti-bearing Steel on the Ductility of Continuous Casting Slab

Abstract: In order to investigate the loss of the ductility of Ti-bearing ship plate steel under 1000 °C, where the ductility begins to reduce rapidly, so the hot ductility of Ti-bearing ship plate steel has been obtained using the Gleeble 1500 thermal-mechanical simulator and also the studies about the effect of grain boundary ferrite films and precipitates containing Ti on the ductility has been carried out. The result showed that the TiN particles precipitating at 950 °C with a larger size and smaller volume fraction cannot effectively suppress the occurrence of recrystallization and the ductility still retains at a high level, although R.A. value presents a certain degree of decline compared with 1000 °C. A large number of smaller Ti(C,N) particles precipitate at 900 °C and can induce the formation of a very small amount of fine grain boundary ferrite, which deteriorates the adhesion strength of the grain boundary, so the R.A. value rapidly reduces to less than 50%. When the temperature falls to close Ae3 (827 °C), the amount of the grain boundary ferrite films increase due to the ferrite phase transformation, but the ferrite film thickness becomes more uneven at the same time, which results in the increase of strain concentration and plays a leading role in causing the decrease of ductility, so the R.A. value has been kept less than 40% as the temperature cooling to 800 °C from 850 °C. When the temperature further decreases, the ductility starts to recover due to the increase of average ferrite film thickness to a greater degree which greatly reduces the strain concentration of the grain boundary.

Keywords: hot ductility, Ti-bearing steel, induced ferrite, ferrite film thickness uniformity, continuous casting slab, precipitate

PACS® (2010). 62.20.fk

***Corresponding author: Guoyu Qian:** State Key Laboratory of Advanced Metallurgy, University of Science and Technology Beijing, Beijing 100083, China. E-mail: qianguoyu_yejin@126.com
Guoguang Cheng: State Key Laboratory of Advanced Metallurgy, University of Science and Technology Beijing, Beijing 100083, China
Zibing Hou: College of Materials Science and Engineering, Chongqing University, Chongqing 400044, China

DOI 10.1515/htmp-2014-0087
Received May 21, 2014; accepted September 27, 2014; published online November 26, 2014

1 Introduction

In order to improve the impact behaviour and welding performance of ship plate steel, small amounts of Ti is often added to steels because Ti containing precipitates are stable up to high temperatures and able to refine the grain structure in the heat affected zone (HAZ) [1]. Nevertheless, the ductility of steels with addition of Ti is general worse than in Ti free C-Mn-Al steels, in other word, the expansion of ductility trough of hot ductility curve to the higher temperature region, which can easily cause the occurrence of surface cracks of slabs [11]. Therefore, many researchers turned to the study of improving the ductility of Ti bearing steel in the temperature range of the straightening operation (700–1000 °C) in continuous casting [2–3]. The composition of Ti and N (Ti/N ratio and [Ti][N] product) and process conditions (test temperature, strain and strain rate etc.) can determine the precipitation of Ti, which has a large influence on the ductility of steel, so a lot of works have been done for understanding the effect of Ti addition on the ductility [4–5]. Many evidences suggest that both a higher Ti/N ratio which ensures the particles containing Ti coarsening and a lower N level (smaller [Ti][N] product) which ensures low volume fraction of Ti-containing particles could lead to better ductility [6–11]. What is more, the best ductility is likely to be given by a high Ti/N (0.02–0.04% Ti) ratio more than 6 and a low N level less than 0.005% [5, 11–15], which can make for reducing the transverse cracking of continuous casting slab. Under this condition of the concentration, the high Ti/N ratio ensure that there is a large amount of Ti in solution favouring the growth of the particles at higher temperatures that favours coarser precipitation distributions; Meanwhile, low N levels reduce the amount of precipitation that can take place, which can not only restrain grain growth at high temperatures (~1350 °C) but also fail to pin

the boundaries long enough for cracks to link up. In addition, Comineli et al. [7] and Abushosha et al. [11] have also pointed out that the decrease of cooling rate is favour of promoting particles coarsening, which could improve the ductility of steel. Although the measurement mentioned above can improve the ductility to some extent, the surface transverse cracks on slab of Ti-bearing steel have yet to be finally eliminated. The reason is that the fine ferrite films at the grain boundary still have great effect on the ductility of steel in addition to the precipitation of Ti. The fine grain boundary ferrite film with smaller strength than austenite is easy to cause the strain concentration during the deformation, which promote the occurrence of intergranular fracture and lead to poor ductility [4, 16, 17]. However, the study about the effect of precipitation of Ti on the ferrite transformation and the grain boundary ferrite on the ductility of slab in the process of continuous casting in Ti bearing steel is seldom reported.

In this paper, in order to further find out the cause of the poor ductility below 1000 °C of ship plate steel with composition of Ti and N (0.0036% N, 0.02% Ti, Ti/N = 6.25, $[Ti][N] = 0.72 \times 10^{-4}$), the quantitative study about the effect of the thickness and uniformity of the grain boundary ferrite films on the ductility of the high temperature region of the ductility trough in the Ti-bearing continuous casting slab was carried out through the measurement of the R.A. curve, quantitative statistics of the precipitation fraction and the thickness of the grain boundary ferrite films, observation of the ferrite morphology, and also the study of precipitation characteristics of Ti. It has important significance to improve the surface quality of continuous casting slab of Ti-bearing ship plate steel.

2 Material and experimental procedure

The steel used in the present study was Ti bearing low-carbon ship plate steel, the chemical composition of this steel is given in Table 1. Cylindrical tensile specimens of 120 mm in length and 10 mm in diameter were machined from continuous casting slab, a Gleeble 1500 thermal-mechanical simulator was employed to perform the hot tensile straining and the hot ductility was determined as

Table 1: Composition of Ti-bearing ship plate steel examined, mass%

C	Si	Mn	P	S	Ti	Al	N
0.16	0.22	1.43	0.015	0.004	0.022	0.031	0.0032

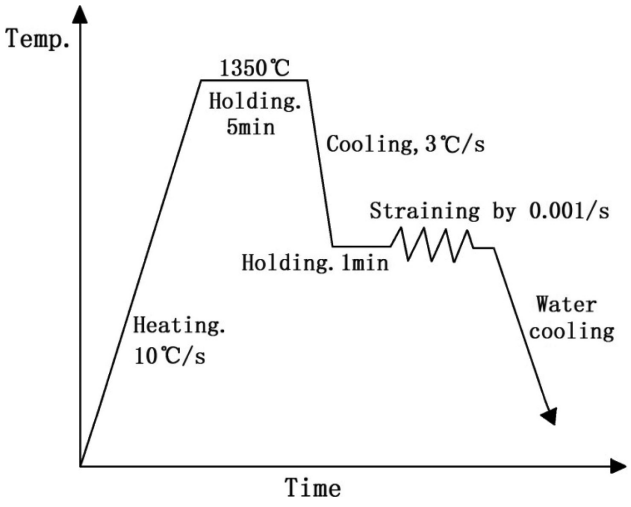

Fig. 1: Thermal schedule used for investigation of hot ductility of Ti-bearing steel.

the reduction of area (R.A.). After the specimens were positioned horizontally and fixed, the argon was inflated into the sample chamber at 1 L/min. The specimens were heated at 10 °C/s to 1350 °C and hold for 5 min followed by direct cooling to test temperature at 3 °C/s. Specimens were held for 60 s at the final testing temperature before stretching straining to failure at the slow strain rate of 0.001 s^{-1}, after fracture the specimens were allowed to rapidly cool by spraying a lot of water to keep the original morphology of fracture surface, the thermal schedule as shown in Fig. 1.

The specimens after tensile test, as shown in Fig. 2(a), were cut off into cylindrical specimens of 10 mm in length on the side of fracture surface. Subsequently, these cylindrical specimens of 10 mm in length were cut off longitudinally, as shown in Fig. 2(b), and then were polished and etched using 4% nital alcohol solution to obtain the metallographic microstructures. With the aid of a Metalloscope, the observation of metallographic microstructures was carried out in the perspective of the magnified 200 times, so 20 fields of microstructure pictures with a side length of 0.6 mm in square were obtained in succession near the fracture region of 3 mm, as shown in Fig. 2(c). Ferrite volume fraction was analyzed by using the ImageJ software to each microstructure picture, and the mean value of the ferrite volume fraction from 20 microstructure pictures was obtained at each test temperature. The thickness and length of the grain boundary ferrite films were measured by using SuperImage software, and the sum of length of ferrite films in each thickness range (0–1 μm, 1–2 μm and 3–4 μm, etc.) and the overall of ferrite films in 20 fields of microstructure pictures at each temperature were obtained through the precise measurement of the thick-

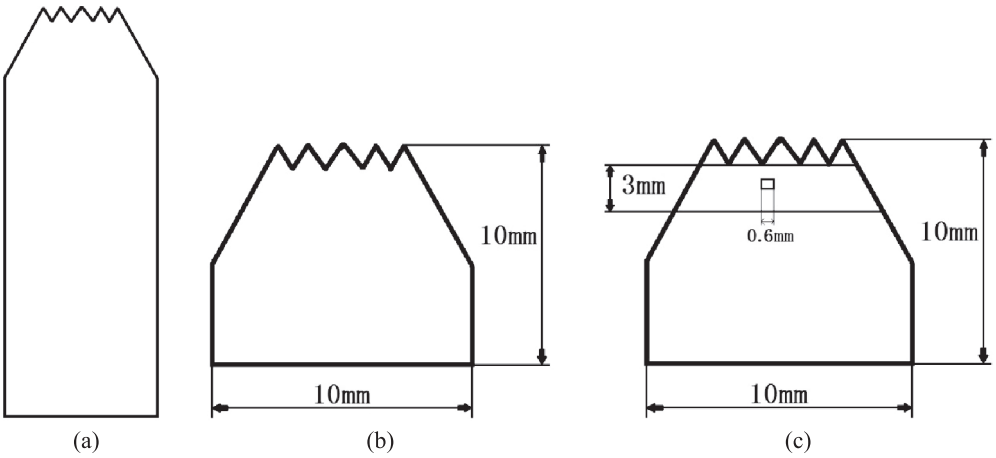

Fig. 2: Schematic diagrams of sample processing showing (a) the specimen after fracture; (b) the specimen near fracture surface; (c) the specimen after polished and etched.

ness and length of the grain boundary ferrite films in all the pictures, where the average thickness and the overall length of grain boundary ferrite films at each temperature as shown in each picture in Fig. 6. It is worth noting that the ferrite films are not completely surrounded by the grain boundaries at 950 °C, so the overall of grain boundaries instead of the overall of the ferrite films were measured and the ferrite film-lack grain boundaries were classified within the thickness range of 0–1 μm. Finally, the frequencies of ferrite films of different thicknesses can be obtained through dividing the sum of length of ferrite films in each thickness range (0–1 μm, 1–2 μm and 3–4 μm, etc.) by the overall of grain boundary ferrite films observed in 20 fields of microstructure pictures at each temperature.

In addition, three square carbon films with 2 mm side length which were used for carbon replicas were taken in 3 mm area adjacent to the fracture surface, the location of these carbon films as shown in Fig. 3. Precipitates were examined by using transmission electron microscope (TEM) at each temperature, and the chemical compositions of precipitates were analyzed using an energy dispersive spectrometer (EDS), 20 fields from three square carbon films at each temperature were selected for determining the size distribution of the numerous precipitates by using the "Soft Imaging System" software of TEM. The equilibrium phase transition temperature (Ae3) of the steel was calculated through Thermal-calc software, and the ferrite transformation starting temperature (Ar3) was measured by dilatometer experiments.

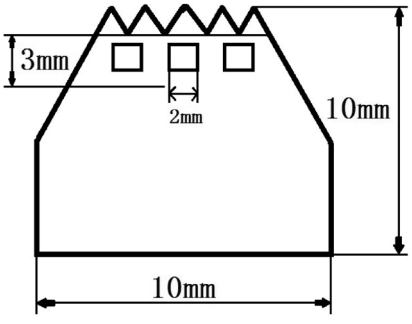

Fig. 3: Schematic diagram showing sampling plan of carbon replicas.

3 Results

3.1 Hot ductility and distribution of ferrite films

3.1.1 Hot ductility and volume fraction of ferrite

The volume fraction of induced grain boundary ferrite and R.A. as a function of temperature for Ti bearing steel are shown in Fig. 4. It can be seen that the R.A. value is more than 90% at 1000 °C and reduces to about 70% as the temperature cooling to 950 °C, which still presents a good ductility. However, the R.A. value rapidly decrease to below 50% which presents a poor ductility when the temperature drops to 900 °C and the precipitation of a small amount of grain boundary ferrite has occurred at the same time. As the process of the temperature further down to 800 °C, the volume fraction of ferrite slowly increases to 8% and the R.A. value has been in a low level (less than 40%). When the temperature further falls to 750 °C, which is close to Ar3 (718 °C), the volume fraction of ferrite increases to 25% and the R.A. value rapidly increases to

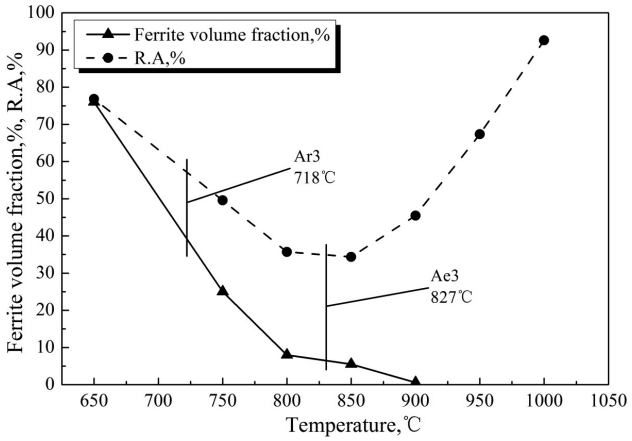

Fig. 4: Ferrite volume fraction and R.A. as a function of temperature in Ti-bearing steel.

more than 50%. At the followed more lower temperature, the volume fraction of ferrite begins to further increase rapidly as the temperature decreases and the R.A. also presents the trend of rapid increase. Finally, the value of ferrite volume fraction and R.A. value increases to 76% and 76.85%, respectively, when the temperature down to 650 °C.

3.1.2 Morphology of ferrite

Figure 5 shows the microstructures of Ti-bearing steel at different temperatures, it can be known that there is no the precipitation of ferrite at the grain boundary at 950 °C. What is more, incomplete grain boundaries resulted from the grain boundary migration are widespread, as shown the area covered with black words at 950 °C in Fig. 5, which indicated the occurrence of dynamic recrystallization. Only a small amount of ferrite films precipitate at some grain boundaries until that the temperature drops to 900 °C, as shown the black arrows at 900 °C in Fig. 5. As the temperature further drops to 850 °C, the thickness of ferrite films becomes heavier and the γ grain boundaries are completely wrapped by them, also the thickness of ferrite films at different positions of the grain boundaries appears to be uneven. The above changing behaviour trend of the grain boundary ferrite films extends to 800 °C, but the ferrite films are still keeping relatively thin at these temperatures. In the process of the temperature cooling to 750 °C from 800 °C, the thickness of ferrite films grows fast and its nonuniformity increases obviously. Ferrite almost accounts for most of the metallographic microstructure at 650 °C due to the occurrence of ferrite phase transformation on a big scale. These grain boundary ferrite films with different thicknesses have significant effect on the ductility, so the thickness distribution and the volume fraction of induced grain boundary ferrite films are to be discussed in detailed.

3.1.3 Thickness of ferrite films

The frequency of grain boundary ferrite films with different thickness as a function of temperature of Ti-bearing steel is shown in Fig. 6 and Fig. 7 presents the average thickness of ferrite films and ferrite volume fraction versus temperature. It is shown that just a small amount of ferrite has already formed at γ boundary when the temperature is above 900 °C and the precipitation of ferrite has not happened at most of the grain boundaries, as shown at 900 °C in Fig. 6. The thickness distribution of ferrite films mainly concentrates in the range of 1 to 4 μm and the average thickness of ferrite films is 2.1 μm at 900 °C. These thin ferrite films with lower strength compared with the austenite can lead to the strain concentration of grain boundary and also suppress the occurrence of recrystallization when the deformation is taking place, so that they can weaken the cohesion of the grain boundary and reduce the ductility of steel. With the temperature decreasing from 900 °C to 850 °C, the thickness and volume fraction of ferrite films gradually increase, but the nonuniformity of the ferrite films thickness raises at the same time. The changing trend of the grain boundary ferrite films continues to 800 °C. However, when the temperature down to near 750 °C which is close to Ar3, ferrite grows up quickly due to ferrite phase transformation. The volume of ferrite and the average thickness of ferrite films quickly increases to about 25% and more than 10 μm, respectively, which is in favor of the improvement of ductility because of the decease of the strain concentration at the grain boundary, although the nonuniformity of the ferrite films thickness further raises.

3.2 Morphology and size distribution of precipitates

3.2.1 Morphology of precipitates

Figure 8 shows the TEM replica micrographs and corresponding EDX spectra at 950 °C and 900 °C in Ti-bearing steel, it can be known that the number of particles is smaller and the size of particles is larger at 950 °C, and the main composition of the particles is TiN according to the EDX spectra. When the temperature cooling to 900 °C,

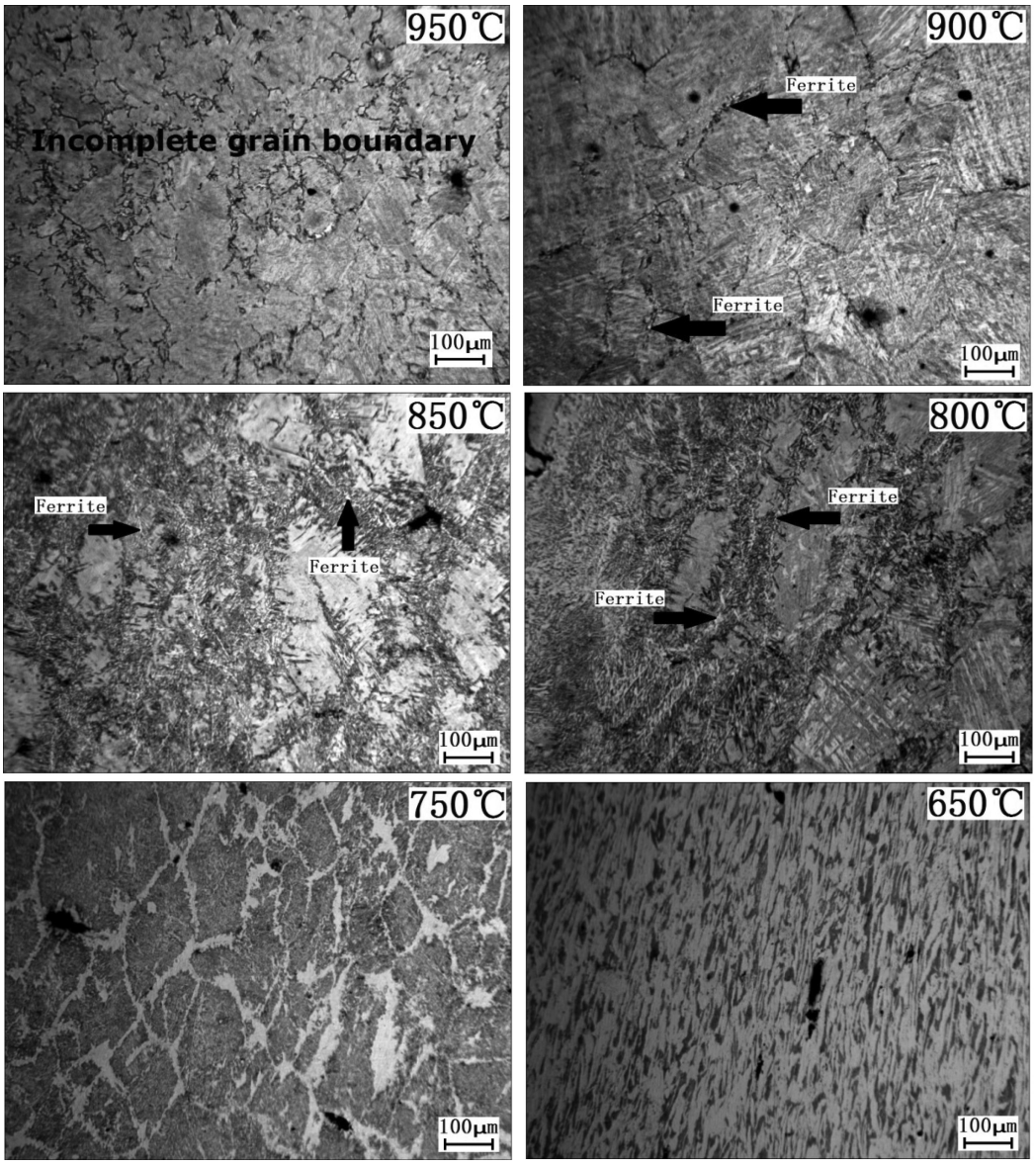

Fig. 5: Microstructure pictures at different temperatures in Ti-bearing steel.

the size of the particles decreases with the increase of the number. According to the others works [4–6], we can know that the TiCN can be detected in the range of temperature in present work and also C was detected in our work, so it is probable for the present of C in our work. Therefore, Ti(C,N) was shown in paper rather than TiCN, and Ti(C,N) means that C may exist, as shown the EDS spectra of 900 °C in Fig. 8. With the temperature down to 850 °C further, both the size and number of particles reduce rapidly, as shown the black arrows of 850 °C in Fig. 9, and it is almost impossible to find out the presence of precipitation particles at 800 °C.

In order to illustrate that the composition (0.022% Ti, 0.0032% N and Ti/N = 6.25) and cooling speed (180 K min^{-1}) in this paper can also lead to the better ductility, the comparison between present work and Abushosha's work [11] has been carried out through the given particle sizes, cooling rates, and reduction of area values, as shown in Table 2. It is worth mentioning that the steel presents a better ductility when the Ti/N ratio is 6.2 compared with the other Ti/N ratio both under lower (25 K min^{-1}) and higher (100 K min^{-1}) cooling rate in Abushosha's work [11]. It can be known through the comparison that the size of particles of present work (15.4 nm) and Abushosha's work (20 nm and 12.5 nm) is very close due to the lower [Ti][N] product of present work, which lead to a better ductility (67%) than Ahushosha's work (55% and 46%), although the cooling rate of present work is larger, as 180 K min^{-1}.

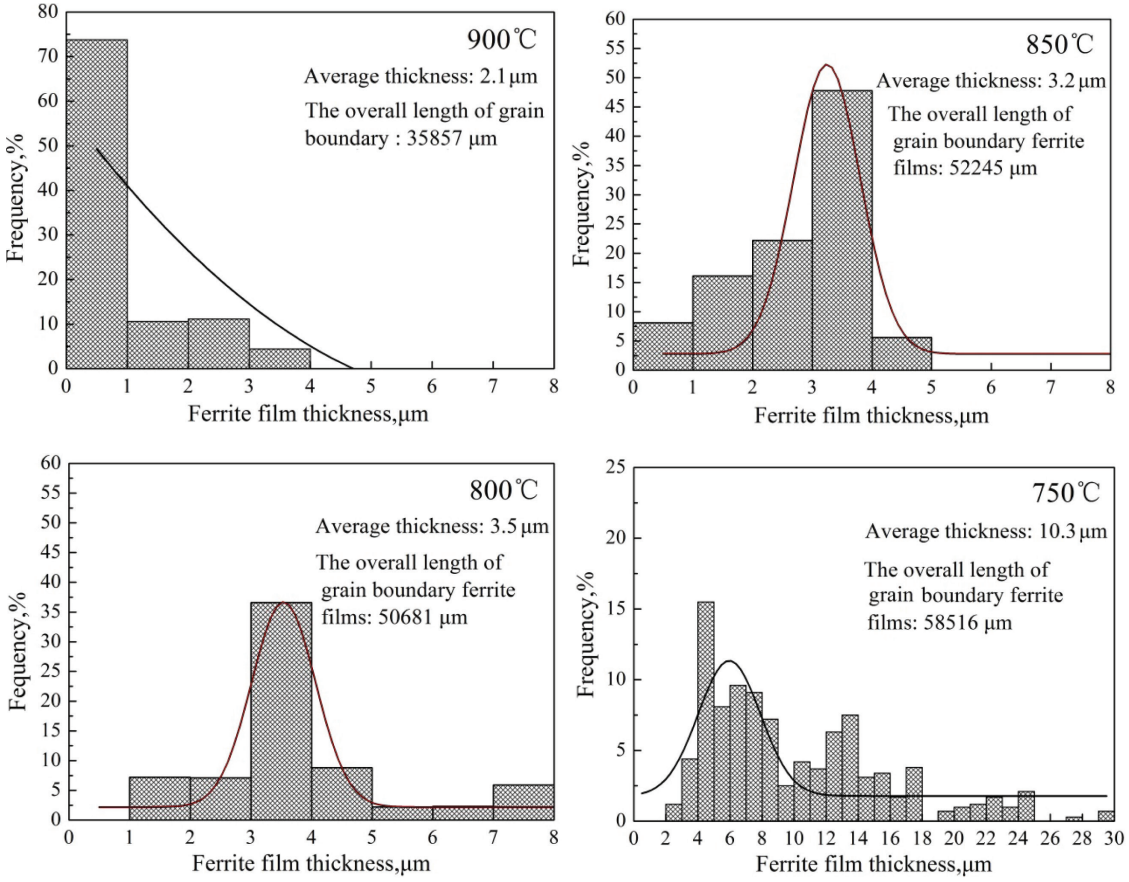

Fig. 6: Frequency of ferrite films as a function of temperature in Ti-bearing steel.

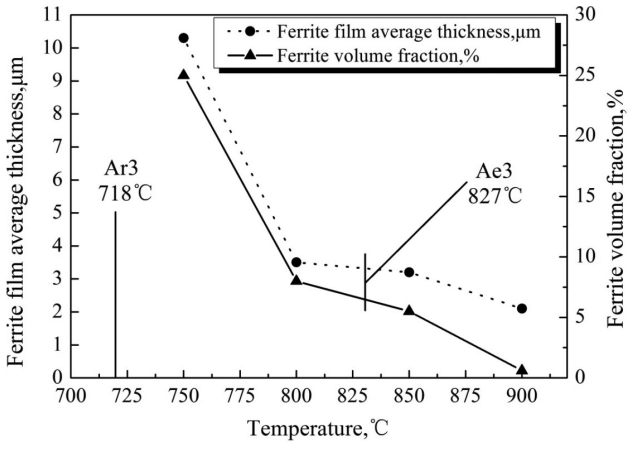

Fig. 7: Ferrite film average thickness and ferrite volume fraction as a function of temperature in Ti-bearing steel.

The size of particles is 11.4 nm at 900 °C in present work, which is close to the size of particles under 100 K min^{-1} in Ahushosha's work at 950 °C, and the R.A. of both is same, as 46%. Therefore, it can be understood that the composition of Ti and N in present work can lead to a good ductility. So it has important significance for further improving the surface quality of slab of Ti bearing ship plate steel by studying the cause of the poor ductility of Ti bearing steel with the composition which favoures the improvement of ductility from the aspects of microstructure under this composition conditions.

3.2.2 The size distribution of precipitates

Figure 10 presents the size distribution of precipitates of Ti-bearing steel as a function of temperature, and these results come from the statistics of precipitates in 20 fields near the fracture area, where the number of particles investigated on the whole at 950 °C, 900 °C and 850 °C, and the minimum target particle size is 1 nm. It can be seen that the size of particles is relatively large at 950 °C and become smaller with the temperature decreasing. The average diameter of the particles was determined through calculation of the size distribution and then the volume fraction of precipitates was calculated out as the average diameter was set into Eq. (1) [18], the results as shown in Fig. 11. Figure 11 shows the average diameter and volume fraction of precipitates of Ti-bearing steel as a function of

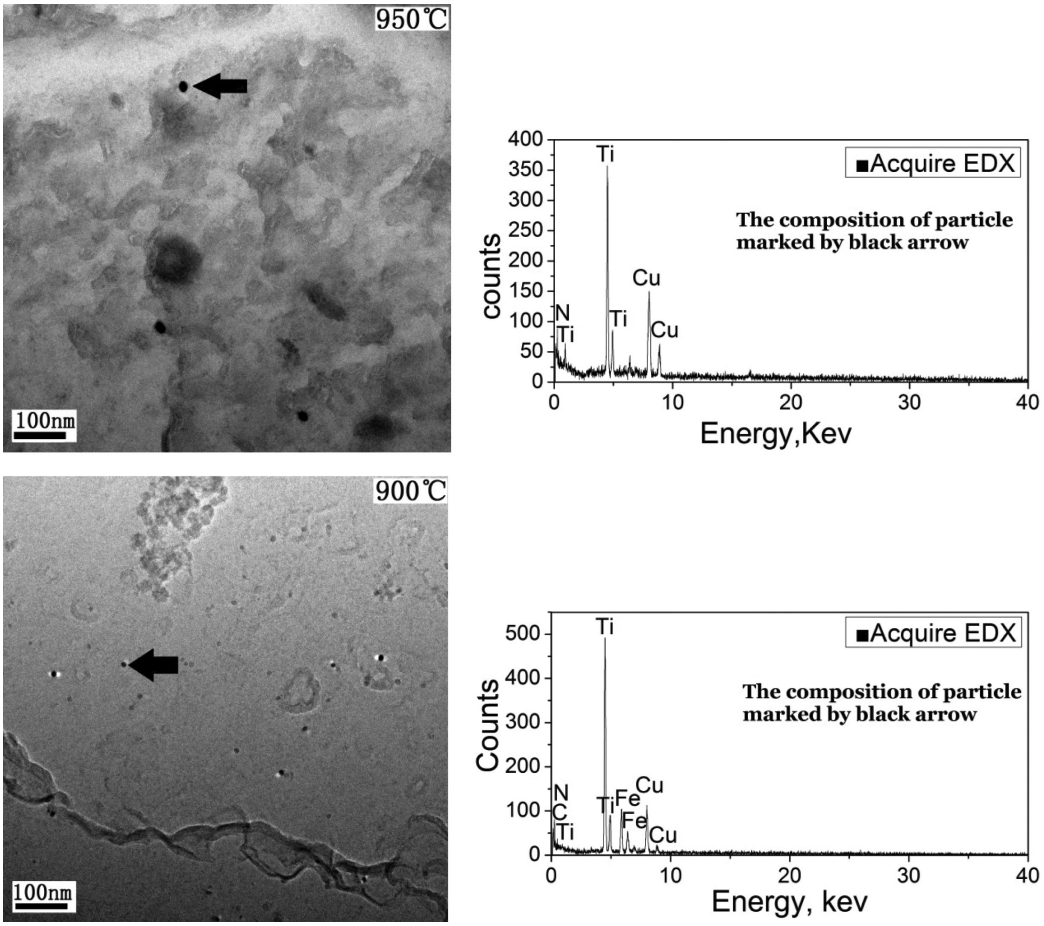

Fig. 8: TEM replica micrographs and corresponding EDX spectra at 950 °C and 900 °C in Ti-bearing steel.

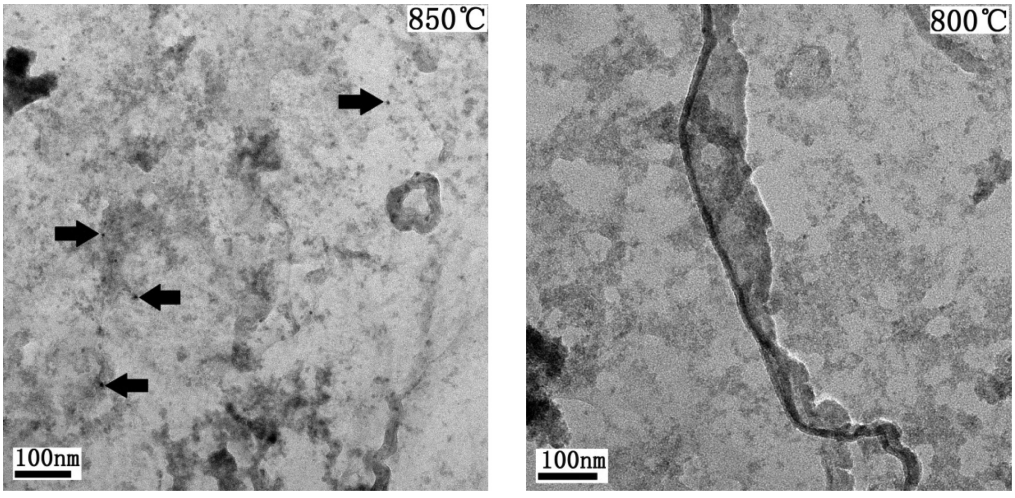

Fig. 9: TEM replica micrographs below 900 °C in Ti-bearing steel.

Table 2: Contrast information of TEM replica micrographs

Work	Temperature (°C)	Cooling rate (K min^{-1})	Particle size (nm)	R.A. (%)	Ti/N	[Ti][N]
Author	950	180	15.4	67	6.25	2.46×10^{-4}
	900	180	11.4	46	6.25	2.46×10^{-4}
Abushosha et al. [1]	950	25	20	55	6.2	0.72×10^{-4}
	950	100	12.5	46	6.2	0.72×10^{-4}

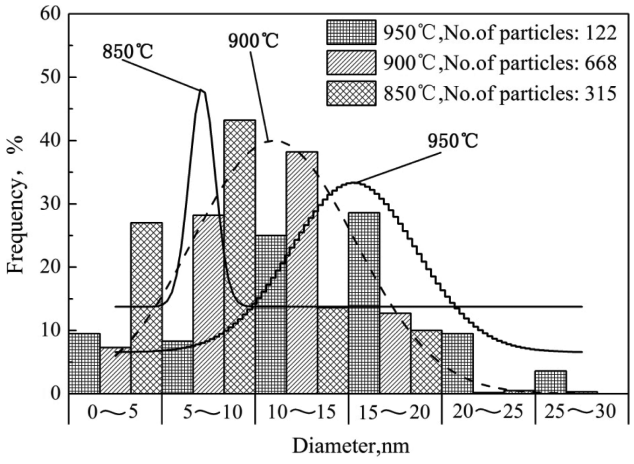

Fig. 10: Size distribution of precipitates as a function of temperature in Ti-bearing steel.

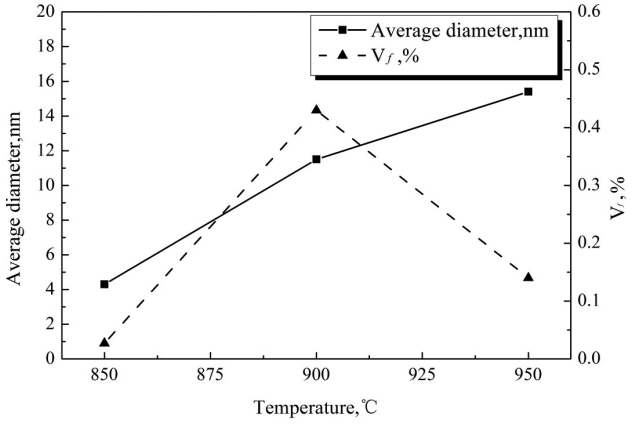

Fig. 11: Average diameter and volume fraction of particles as a function of temperature in Ti-bearing steel.

temperature, and it is indicated that the average diameter of particles is relatively large at 950 °C (15.4 nm), although the volume fraction of precipitates is very small (only 0.14%). The average diameter of particles decreases as the temperature decreases and reduces to only 4.3 nm at 850 °C. However, the volume fraction of precipitates gradually increases as the temperature cooling from 950 °C to 900 °C and rapidly reduces to only 0.027% at 850 °C [18].

$$V_f = \left[\frac{1.4\pi}{6}\right] \times \left[\frac{ND^2}{A}\right] \quad (1)$$

where D is the average diameter of particles, N is the number of precipitates and A is the area of field observed.

4 Discussion

As shown in Fig. 10 and Fig. 11, it can be known that the TiN particles precipitating at 950 °C have a relatively larger size (average diameter 15.4 nm) and relatively smaller volume fraction (0.14%) and they cannot effectively suppress the occurrence of recrystallization, as shown the picture of 950 °C in Fig. 5 where partial recrystallization happens, which lead to a good ductility and the R.A. value is about 70%. When the temperature falls to 900 °C, a large number of smaller Ti(C,N) particles begin to precipitate, the average diameter and volume fraction of them is 11.5 nm and 0.43%, respectively. In this case, the interfacial energy of γ grain boundary ($\sigma_{\gamma\gamma}$) is raised because of the precipitation of these fine Ti(C,N) particles in the neighborhood of grain boundaries, according to Eq. (2), which lead to the rapid increase of the nucleation rate of ferrite ($\dot{N}$) on the γ grain boundaries. Figure 8 shows that there are some particles in the neighborhood of grain boundaries. Therefore, the precipitation of a small amount of fine ferrite at γ grain boundaries occurs at higher temperature above Ae3, as shown in Fig. 6 and Fig. 7 [19].

$$\dot{N} = C \exp\left\{-\left[\frac{(3\sigma_{\gamma\alpha} - \sigma_{\gamma\gamma})^3}{3(\Delta F + W)^2} + \Delta F_D\right] / RT\right\} \quad (2)$$

where $\dot{N}$ is the nucleation rate of ferrite on the γ grain boundaries; C is constant; $\sigma_{\gamma\alpha}$ and $\sigma_{\gamma\gamma}$ are interfacial free energy of γ-α, γ-γ; ΔF is free energy change in transfor-

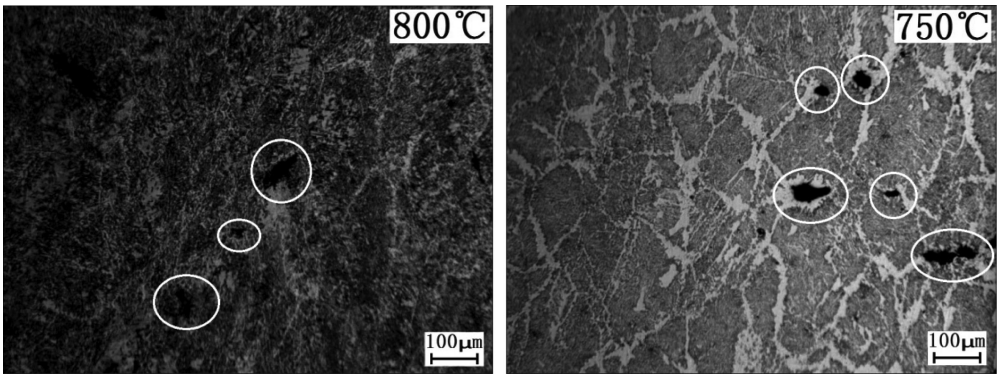

Fig. 12: Microstructure pictures at 800 °C and 750 °C in Ti-bearing steel.

mation; W is volume strain energy associated with transformation; ΔF_D is activation energy of diffusion of C atom in γ.

These fine Ti(C,N) particles and a small amount of ferrite can play a role in pinning the γ grain boundary, which can hinder the migration of the grain boundary. At the same time, the driving forces of grain growth become smaller when the temperature down to below 1000 °C [20, 21]. In addition, the work of Chapa et al. [22] shows that the pining forces of Ti-bearing precipitates are always greater than or equal to the driving forces of grain boundary at 900 °C, where the Ti content and size of Ti-bearing precipitates in the work of Chapa and the present paper almost have the same value. So it can be known that the fine Ti(C,N) particles at boundaries can suppress the migration of grain boundaries and the occurrence of recrystallization, which promote the grain boundary sliding and the emergence of the grain boundary microvoid, and then can lead to the rapid reduce of the value of R.A. (less than 50%) at 900 °C. As the temperature cooling to 850 °C (close to Ae3), the grain boundary ferrite increases and surrounds the whole boundaries, so these fine ferrite films can cause strain concentration at boundary, which leads to the further decrease of the value of R.A. (less than 40%), though the size and volume fraction of precipitates become smaller. With the temperature cooling from 850 °C to 800 °C (under Ae3), the grain boundary ferrite films further increase due to the phase transformation of ferrite, meanwhile, the nonuniformity of ferrite thickness becomes serious, which would have an influence on the strain concentration at grain boundary. The nonuniform grain boundary ferrite films can cause uneven stress distribution around the austenite grain boundary when a tensile force is imposed on the austenite grain boundary, which will lead to the increase of local stress concentration, so the source of crack may occur where the stress is larger. Once the source of crack appears and it can be easy to develop a crack when the tensile force is kept. This effect may be illustrate in some degree from Fig. 12, it can be seen that cracks are easy to generate at the fork points where the stress concentration is larger and the thickness of ferrite film is bigger, as shown the white circles in Fig. 12. The increase of strain concentration results from the uneven grain boundary ferrite films plays a leading role in deteriorating the ductility of steel, although the average thickness of ferrite films increases slowly with temperature cooling in this temperature range, as shown in Fig. 7, which is favor of relieving the strain concentration and improving the ductility to some extent. When the temperature further down to close Ar3 (718 °C), the occurrence of ferrite transformation is on a big scale, so the increase of average thickness to a greater degree, which greatly reduces the strain concentration of the grain boundary, although the nonuniformity of ferrite films thickness is still larger, as shown the 750 °C in Fig. 6 and Fig. 7. Finally, the ductility starts to recover and increases to more than 50% and 75% when the temperature cools to 750 °C and 650 °C, respectively.

5 Conclusions

1. The value of R.A. in Ti-bearing ship plate steel decreases rapidly when the temperature falls to 950 °C from 1000 °C, but still retains at a high level (70%). The R.A. value further rapidly reduces to less than 50% as the temperature down to 900 °C. In the process of temperature reduce to 800 °C from 850 °C, the R.A. value has remained less than 40%. As the temperature further decreases, the ductility begins to recover.
2. Partial recrystallization happens at 950 °C and a very small amount of ferrite has not precipitated at grain boundary until the temperature falls to 900 °C. As the temperature decreases, along with the increase of the

average thickness of ferrite films and the nonuniformity of ferrite film thickness increases at the same time.

3. The average diameter of TiN particles is relatively large at 950 °C (15.4 nm) and their volume fraction is very small (only 0.14%). When the temperature down to 900 °C, the particles is mainly composed of Ti(C,N) and their average diameter further decreases compared with 950 °C and reduces to only 4.3 nm at 850 °C. Nevertheless, the volume fraction of precipitation particles containing Ti gradually increases as the temperature cooling from 950 °C to 900 °C and rapidly reduces to only 0.027% at 850 °C. As the temperature further decreases, the precipitates become rare.
4. The TiN particles precipitating at 950 °C with a larger size and a smaller volume fraction cannot effectively suppress the occurrence of recrystallization and the ductility still retains at a high level. A large number of smaller Ti(C,N) particles precipitate at 900 °C and can induce the precipitation of a very small amount of fine grain boundary ferrite, which deteriorate the adhesion strength of the grain boundary, so the R.A. value rapidly reduces to less than 50%. When the temperature falls to close Ae3, the amount of the grain boundary ferrite films increase due to the ferrite phase transformation and the nonuniformity of ferrite film thickness becomes serious at the same time, which results in the increase of strain concentration and plays a leading role in leading to the decrease of ductility, so the R.A. value has been kept less than 40% as the temperature cooling to 800 °C from 850 °C. When the temperature further decreases, the ductility starts to recover due to the increase of average thickness to a greater degree which greatly reduces the strain concentration of the grain boundaries.

Acknowledgments: The authors would like to be grateful to the National Natural Science Foundation of China (No. 51374020) and every student in our lab for their assistance in the experiment.

References

[1] M. A. Linaza, J. L. Romero, J. M. Rodergues Ibabe and J. J. Urcola: *Mech. Work. Steel Process. Conf.*, 36(1995) 483–494.
[2] C. Ouchi and K. Matsumoto: *Trans. Iron Steel Inst. Jpn.*, 22(1982) 181–189.
[3] R. Abushosha, R. Vipond and B. Mintz: *Mater. Sci. Technol.*, 7(1991) 613–620.
[4] B. Mintz, S. Vue and J. J. Jonas: *Int. Mater. Rev.*, 36(1991) 187–220.
[5] B. Mintz: *ISIJ Int.*, 39(1999) 833–855.
[6] B. Mintz and D. N. Crowther: *Int. Mater. Rev.*, 55(2010) 168–196.
[7] O. Comineli, R. Abushosha and B. Mintz: *Mater. Sci. Technol.*, 15(1999) 1058–1067.
[8] B. Mintz: *Ironmaking Steelmaking*, 27(2000) 343–347.
[9] R. Abushosha, R. Vipond and B. Mintz: *Mater. Sci. Technol.*, 7(1991) 613–620.
[10] C. Spradbery and B. Mintz: *Ironmaking Steelmaking*, 32(2005) 319–324.
[11] R. Abushosha, O. Comineli and B. Mintz: *Mater. Sci. Technol.*, 15(1999) 278–286.
[12] H. Luo, L. Pentti Karjalainen, D. A. Porter and H. M. Liimatainen: *ISIJ Int.*, 42(2002) 273–282.
[13] T. H. Coleman and J. R. Wilcox: *Mater. Sci. Technol.*, 1(1985) 80–89.
[14] E. T. Turkdogan: AIME Steelmaking Conf. Proc., Warrendale, PA, 70(1987) 399–408.
[15] M. Hater, R. Klages, B. Redenz and K. Taffner: Open Hearth Proc., AIME, Warrendale, (1973) 202–211.
[16] A. Cowley, R. Abushosha and B. Mintz: *Mater. Sci. Technol.*, 14(1998) 1145–1153.
[17] Y. Maehare, K. Yasumoto, H. Tomono, T. Nagamichi and Y. Ohmori: *Mater. Sci. Technol.*, 6(1990) 793–806.
[18] H. Ma and Y. Li: *Mater. Sci. Eng.*, 20(2002) 328–337.
[19] C. Ouchi, T. Sampei and I. Kozasu: *Transaction ISIJ*, 22(1982) 214–222.
[20] M. I. Vega, S. F. Medina, A. Quispe, M. Gómez and P. P. Gómez: *ISIJ Int.*, 45(2005) 1878–1886.
[21] S. F. Medina, M. I. Vega, M. Gómez and P. P. Gómez: *ISIJ Int.*, 45(2005) 1307–1315.
[22] M. Chapa, S. F. Medina, V. López and B. Fernández: *ISIJ Int.*, 42(2002) 1288–1296.